HYPERAUTOFLUORESCENT RING IN AUTOIMMUNE RETINOPATHY

LUIZ H. LIMA, MD[*,†], **JONATHAN P. GREENBERG, MD**[‡,§,¶], **VIVIENNE C. GREENSTEIN, PhD**[¶], **R. THEODORE SMITH, MD, PhD**[¶], **JULIANA M. F. SALLUM, MD**[†], **CHARLES THIRKILL, PhD**[**], **LAWRENCE A. YANNUZZI, MD**[*], and **STEPHEN H. TSANG, MD, PhD**[‡,§,¶]

[*]Vitreous, Retina, Macula Consultants of New York and The LuEsther T. Mertz Retinal Research Center, Manhattan Eye, Ear, and Throat Hospital, New York, New York

[†]Department of Ophthalmology, Federal University of Sao Paulo (UNIFESP), Sao Paulo, Brazil

[‡]Bernard and Shirlee Brown Glaucoma Laboratory, Edward S. Harkness Eye Institute, Columbia University, New York, New York

[§]Department of Pathology and Cell Biology, Columbia University, New York, New York

[¶]Department of Ophthalmology, Columbia University, New York, New York

[**]Department of Ophthalmology, University of California, Davis, California

Abstract

Purpose—To report the presence of a hyperautofluorescent ring and corresponding spectral-domain optical coherence tomography (SD-OCT) features seen in patients with autoimmune retinopathy.

Methods—All eyes were evaluated by funduscopic examination, full-fleld electroretinography, fundus autofluorescence, and SD-OCT. Further confirmation of the diagnosis was obtained with immunoblot and immunohistochemistry testing of the patient's serum. Humphrey visual fields and microperimetry were also performed.

Results—Funduscopic examination showed atrophic retinal pigment epithelium (RPE) associated with retinal artery narrowing but without pigment deposits. The scotopic and photopic full-field electroretinograms were nondetectable in three patients and showed a cone–rod pattern of dysfunction in one patient. Fundus autofluorescence revealed a hyperautofluorescent ring in the parafoveal region, and the corresponding SD-OCT demonstrated loss of the photoreceptor inner segment–outer segment junction with thinning of the outer nuclear layer from the region of the hyperautofluorescent ring toward the retinal periphery. The retinal layers were generally intact within the hyperautofluorescent ring, although the inner segment–outer segment junction was disrupted, and the outer nuclear layer and photoreceptor outer segment layer were thinned.

Conclusion—This case series revealed the structure of the hyperautofluorescent ring in autoimmune retinopathy using SD-OCT. Fundus autofluorescence and SD-OCT may aid in the diagnosis of autoimmune retinopathy and may serve as a tool to monitor its progression.

Keywords

autoimmune retinopathy; cancer-associated retinopathy; fundus autofluorescence; hyperautofluorescent ring; inner segment–outer segment junction; spectral-domain optical coherence tomography

Autoimmune retinopathies (AIRs), including cancer-associated retinopathy, melanoma-associated retinopathy, and nonparaneoplastic AIR, are rare and highly heterogeneous syndromes that may produce different ocular symptoms. They may be related to diverse malignancies, such as lung, prostate, breast, colon, gynecologic, and hematologic cancers, including leukemias, myelomas, and lymphomas. However, small-cell lung cancer is the systemic malignancy most often associated with cancer-associated retinopathy.[1–4] Although the diagnosis of AIR is suggested by the combination of rapid and progressive deterioration in visual function, decreased electroretinography (ERG) responses out of proportion to clinical features, and the presence of circulating antiretinal autoantibodies,[3] the diagnosis of AIR can be challenging. Although the antibodies against recoverin and α-enolase are the most common antibodies associated with AIR, various other causative antibodies have been described.[1,3,5,6] Additionally, antiretinal antibodies have been described in other disorders, such as acute zonal occult outer retinopathy (AZOOR)[7,8] and retinitis pigmentosa (RP), especially in the presence of bilateral macular edema.[9,10] They are frequently observed in normal patients as well.[11] Therefore, the role of antiretinal antibodies for the diagnosis of AIR remains unclear.

Fundus autofluorescence (FAF), a noninvasive technique that uses a scanning laser ophthalmoscope, has been performed as an important tool in the examination of acquired and inherited retinal diseases.[12–16] This procedure allows for the evaluation of lipofuscin, which is the major fluorophore derived from photoreceptor outer segments, before it accumulates in the pigment epithelial cells.[17] Decreased autofluorescence (hypoautofluorescence) may indicate photoreceptor death and retinal pigment epithelial (RPE) atrophy, and increased auto-fluorescence (hyperautofluorescence) suggests compromised RPE function related to an ongoing metabolic demand, without or before photoreceptor degeneration.[10,18] The abnormal parafoveal accumulation of lipofuscin represented by a hyperautofluorescent ring may be a precursor of apoptosis and has been suggested as having prognosticating value because it can constrict in patients with RP.[19,20] In addition to RP, hyperautofluorescent rings have been described in other retinal degenerative diseases, such as cone dystrophy, X-linked retinoschisis, and Leber congenital amaurosis.[21–23] We report hyperautofluorescent rings and corresponding spectral-domain optical coherence tomography (SD-OCT) findings in four cases of AIR.

Methods

The Institutional Review Board/Ethics Committee approval was obtained for this study (IRB-AAAE1564; approval: June 26, 2009; expiration: April 4, 2011). Over a 2-year period,

4 patients with AIR were diagnosed and enrolled at the Columbia University Medical Center/New York Presbyterian Hospital.

The history, symptoms, funduscopic examination, and full-field ERG were supportive of the diagnosis of AIR. Full-field ERGs (Diagnosys LLC, Lowell, MA) were recorded from both eyes with DTL electrodes according to the International Society for Clinical Electrophysiology of Vision standard in both scotopic and photopic states.[24] Further confirmation was obtained with 1:500 dilutions immunoblot and immunohistochemistry (IHC) testing of the patient's serum, which were performed as previously described.[3,5]

Fundus autofluorescence and SD-OCT imaging (Spectralis SD-OCT-SLO; Heidelberg Engineering, Heidelberg, Germany) were performed in all four cases, and the images were automatically aligned by the Heidelberg Eye Explorer software. For Patients 2, 3, and 4, horizontal distances were measured from the fovea to the inner and outer borders of the hyper-autofluorescent rings. This measurement was performed using the ruler tool available on Adobe Photoshop (Photoshop CS3; Adobe Systems, Inc, San Jose, CA). The average horizontal distance between the fovea and the inner borders of the hyperautofluorescent ring was divided by the total image width (millimeters). Each FAF image was a 30° field, so the obtained fractions were multiplied by 30 to convert them into degrees. The same measurements were performed for the outer borders of the hyperautofluorescent ring.

All cases were tested with standard automatic perimetry using the Humphrey Visual Field (HVF) analyzer (Humphrey Systems, Dublin, CA), stimulus size III, 24-2 grid. Microperimetry (MP1) (10-2 pattern; NAVIS software version 1.7.3; Nidek Instruments, Inc, Padova, Italy) was performed in Patients 2 and 3, and the results were superimposed on the corresponding FAF images using the microperimeter's built-in registration software.

Results

Patient 1

An 82-year-old man presented with photopsias and decreased peripheral vision of 5-month duration, followed shortly by decreased central vision in both eyes. His medical history included a late-stage small-cell lung cancer, which was diagnosed 3 months after the onset of his visual symptoms, and he was treated with chemotherapy (carboplatin/etoposide). He had been smoking at least 1 pack of cigarettes a day for 30 years. His medication consisted of furosemide and escitalopram. Best-corrected visual acuity was count fingers at 5 ft in both eyes. Anterior segment examination was unremarkable, except for pseudophakia. The funduscopic examination revealed cellular reaction in the vitreous, retinal artery narrowing, atrophic RPE changes with fine peripheral white dots, and RPE mottling in both eyes. No disc pallor or intraretinal pigment migration was noted. Fundus autofluorescence showed a hyperautofluorescent ring in the macular area of both eyes. Spectral-domain optical coherence tomography imaging demonstrated changes in retinal structure that corresponded to inner segment–outer segment (IS–OS) junction loss and outer nuclear layer (ONL) thinning over the hyperautofluorescent transition zone. The retinal structure was generally intact within the hyperautofluorescent ring, but there was marked thinning of the ONL and disruption of the IS–OS junction toward the inner border of the ring. Thinning of the

photoreceptor outer segment layer was also observed. Outside the hyperautofluorescent ring, there was IS–OS junction, external limiting membrane (ELM), and ONL loss (Figure 1). The 24-2 HVF showed complete field loss except for the foveal location where sensitivity was markedly decreased (12 dB). Scotopic and photopic full-field ERGs were nonrecordable (Figure 5). Immunoblot analysis showed reactivity against 40-kDa protein (Figure 6), and IHC revealed reactivity against the outer plexiform layer of a primate specimen.

Patient 2

A 61-year-old woman presented with photopsias and central vision deterioration in both eyes over the past 6 months. She had first noticed decreased peripheral vision approximately 18 months before the central vision was affected. Her medical history was noted for psoriasis. There was no smoking history. Best-corrected visual acuity was 20/150 in both eyes. Anterior segment examination was unremarkable. The funduscopic examination revealed cellular reaction in the vitreous, extensive mottling of the RPE, and temporal pallor of the optic disc in both eyes. No intraretinal pigment migration was noted. Fundus autofluorescence showed patchy hypoautofluorescence in the periphery and a hyperautofluorescent ring in the macular area of both eyes. Spectral-domain optical coherence tomography demonstrated IS–OS junction loss, ELM disorganization, and ONL thinning over the hyperautofluorescent transition zone. All retinal layers were present within the hyperautofluorescent ring, but there was discontinuity of IS–OS junction and thinning of the ONL and photoreceptor outer segment layer. Outside the hyperautofluorescent ring, there was loss of the IS–OS junction and ELM and further thinning of the ONL (Figure 2). The inner and outer borders of the hyperautofluorescent ring were located around 1.5° and 5°, respectively, from the fovea in the horizontal mid-line. The 24-2 HVF demonstrated a dense scotoma outside the central 3°, which showed markedly decreased sensitivity. There was decreased sensitivity in the central 3°, and foveal sensitivity was also decreased (26 dB) (Figure 2). The MP1 demonstrated a marked decrease in sensitivity at the inner border of the ring, and sensitivity was nonrecordable outside the ring. Inside the ring, the sensitivity was also decreased (Figure 2). As in Patient 1, scotopic and photopic full-field ERGs were nonrecordable (Figure 5). Immunoblot analysis showed reactivity against 33-, 45-, 55-, 64-, 72-, and 90-kDa proteins, and IHC revealed reactivity against the outer segments as well as the retinal and choroidal vascular beds of a primate specimen (Figure 6).

Patient 3

A 66-year-old man presented with photopsias and decreased central vision in both eyes for 6 months. He noted an initial decrease in peripheral vision before central vision was affected. His medical history did not include any malignancies or tobacco use. Best-corrected visual acuity was 20/25 in the right eye but was 20/50 in the left eye, which demonstrated cystoid macular edema. Anterior segment examination was unremarkable. The funduscopic examination revealed cellular reaction in the vitreous, atrophic RPE changes with retinal artery narrowing, and lack of intraretinal pigment migration in both eyes. Fundus autofluorescence showed large patches of hypoautofluorescence around the inferior arterial arcade with a hyperautofluorescent ring in the macular area. Spectral-domain optical coherence tomography demonstrated IS–OS junction loss and ONL thinning over the hyperautofluorescent transition zone. The retinal structure was generally intact within the

hyperautofluorescent ring, but there were thinning of the ONL and photoreceptor outer segment layer and some disruption of the IS–OS junction toward the inner boundary of the ring. Outside the hyperautofluorescent ring, there was loss of IS–OS junction and ELM, as well as further thinning of ONL (Figure 3). The inner and outer borders of the hyperautofluorescent ring were located around 6° and 7°, respectively, from the fovea in the horizontal mid-line. The 24-2 HVF demonstrated a pattern suggestive of a ring scotoma, with greater sparing of the inferior field that corresponded to the superior fundus. Sensitivity was decreased in the central 5°, and foveal sensitivity was also decreased (33 dB). The MP1 demonstrated a decrease in sensitivity across the horizontal midline, and there was an additional decrease starting at the inner border of the ring. Sensitivity was nonrecordable outside the ring (Figure 3). As was shown on the HVF, the MP1 demonstrated greater sparing of sensitivity associated with the superior retinal locations. The full-field ERG showed reduced scotopic and photopic response amplitudes and a 3-millisecond delay in cone 30-Hz flicker implicit time (Figure 5). Immunoblot analysis showed reactivity against 40-kDa protein, and IHC revealed reactivity against the outer plexiform layer of a primate specimen (Figure 6).

Patient 4

A 70-year-old woman presented with a history of nyctalopia and photopsias for the past 12 months. Her medical history included small-cell lung cancer with occipital lobe metastasis, which was discovered 4 months before the onset of visual symptoms. She was treated with chemotherapy and was in remission at her most recent visit. She had a 20–pack-year smoking history. At her earliest visit, best-corrected visual acuity was 20/30 in both eyes. Anterior segment examination was unremarkable, except for pseudophakia. The funduscopic examination revealed a cellular reaction in the vitreous, mild RPE changes with RPE mottling, and papillophlebitis with swelling of the optic nerve in both eyes. No intraretinal pigment migration was noted. Fundus autofluorescence showed patchy hypoautofluorescence in the periphery and a hyperautofluorescent ring in the macular area. Spectral-domain optical coherence tomography demonstrated IS–OS junction loss and ONL thinning over the hyperautofluorescent transition zone. The retinal structure was generally intact within the hyperautofluorescent ring, but there was thinning of the ONL and photoreceptor outer segment layer and disruption of the IS–OS junction toward the inner boundary of the ring. Outside the hyperautofluorescent ring, there was loss of IS–OS junction and ELM, as well as further thinning of ONL (Figure 4). At her first visit, the inner and outer borders of the hyperautofluorescent ring were located around 4° and 6°, respectively, from the fovea in the horizontal midline. The 24-2 HVF demonstrated dense ring scotoma approximately 9° from the fovea, with the central area exhibiting reduced sensitivity. Three years later, at her most recent visit, her best-corrected visual acuity had decreased from 20/30 to 20/40 in both eyes. Identical SD-OCT sections for her first and last visits were obtained by using the OCT "progression" mode (Spectralis SD-OCT-SLO; Heidelberg Engineering). Over the 3-year period, we observed constriction of both the inner and the outer boundaries of the hyperautofluorescent ring as well as corresponding loss of the IS–OS junction (Figure 4) and an increase in the depth and extent of the scotoma on HVF (Figure 4). There was also a decrease in thickness of the photoreceptor outer segment layer over this period. The foveal sensitivity was decreased at her most recent visit (32 dB).

Scotopic and photopic full-field ERGs were nonrecordable (Figure 5). Immunoblot analysis showed reactivity against 47-kDa protein (Figure 6), and IHC revealed reactivity against inner limiting membrane, inner plexiform layer, and ganglion cell layers of a primate specimen.

Discussion

Autoimmune retinopathy may be present in patients who develop sudden or subacute loss of vision associated with an abnormal ERG and positivity of autoantibodies against retinal proteins. The identification of a malignancy, as in Patients 1 and 4, indicates the diagnosis of cancer-associated retinopathy. Nevertheless, information on the specificity of autoantibodies in AIR patients and their relationship with clinical symptoms is incomplete. In the majority of cases, the diagnosis of AIR is challenging because the symptoms are often disproportionate to the clinical findings, with funduscopic examination revealing only subtle peripheral changes.

In addition to AIR, the clinical history of decreased peripheral vision, followed by decreased central visual acuity, and the funduscopic examination of RPE mottling and atrophy with retinal artery narrowing observed in our study patients can be found in other retinal degenerations, such as RP and late-onset retinal degeneration.[25,26] Additionally, the late-onset presentation observed in our patients can be seen in RP because RP disease expression is variable. However, in such diseases, retinal deterioration is slower than in AIR with a more preserved full-field ERG. In our series, the study patients demonstrated rapid progression of their symptoms, with severely constricted visual fields and decreased central vision within 1 year of symptom onset for Patients 1, 3, and 4 and within 2 years of symptom onset for Patient 2. The degree of vision loss was disproportionate to the subtle funduscopic changes. Additionally, three of the four study patients had nonrecordable ERGs. Patient 3 presented with recordable ERG responses, in keeping with his earlier disease appearance; however, the ERG decrease represented a cone–rod dysfunction, which can be seen more frequently in AIR than in RP.[3,27–29]

All patients were positive for antiretinal antibodies known to be associated with AIR, and their IHCs revealed reactivity against retinal layers and, in Patient 2, against retinal and choroidal blood vessels. None of our patients were proven positive for antibodies against recoverin or α-enolase, which are the most common antiretinal antibodies associated with AIR. However, Weleber et al[27] found antienolase and/or antirecoverin antibodies in less than half of their AIR study patients. Additionally, Patients 2 and 4 demonstrated reactivity against 45-kDa and 47-kDa proteins, respectively. In light of the 1-kDa resolution limit of the immunoblot technique, the activity in either case may have been against α-enolase.

In all four study patients, FAF revealed a parafoveal ring of abnormally enhanced autofluorescence located between an area of apparently normal autofluorescence inside the ring and the hypoautofluorescent retina outside the ring. Spectral-domain optical coherence tomography revealed disorganization and loss of IS–OS junction as well as thinning of ONL over the hyperautofluorescent transition zone. Outside the hyperautofluorescent ring, there was loss of the IS–OS junction and ELM, as well as further thinning and loss of the ONL.

Within the hyperautofluorescent ring, all retinal layers were observed, but there was thinning of the photoreceptor outer segment layer across the central macular region. The 24-2 HVFs provided some evidence of agreement between visual function and the FAF and SD-OCT findings of this study. The extensive scotoma found in three study patients, showing markedly decreased visual function in the same region as the hyperautofluorescent ring, supports the finding of a hyperautofluorescent ring with its corresponding breakdown on SD-OCT. Central and foveal sensitivities were decreased, and these findings are probably because of a loss of photoreceptor outer segments across the central macular area in the study eyes. Patient 4 showed additional loss of photoreceptor outer segments over time as well as a corresponding further reduction of best-corrected visual acuity and of visual sensitivity within the hyperautofluorescent ring. The MP1 was performed in 2 patients, and the results provide further support for an agreement between visual function and the hyperautofluorescent ring. Sensitivity was decreased within the ring and was further decreased at the inner border of the ring, becoming nonrecordable outside the ring.

Our findings in AIR are consistent with previous studies analyzing the structure of hyperautofluorescent ring in RP patients.[20,30] It is hypothesized that, in such patients, the hyperautofluorescent ring represents an anomalous parafoveal collection of lipofuscin in the RPE because of an enhanced outer segment turnover during apoptosis.[20] Because early disorganization of the IS–OS junction lamina is considered a morphologic marker for photoreceptor impairment in human[31,32] and animal models,[33,34] the loss of the IS–OS junction at the transition zone of the hyperautofluorescent ring observed in this case series suggests that the photoreceptor cilia, that is, the IS–OS junction, is likely to be affected by the initial triggers of apoptosis. Similarly to RP, the apoptosis leading to retinal degeneration begins in the retinal periphery in AIR cases.[35]

Although the estimated incidence of hyperautofluorescent rings in RP is between 59% and 94%,[30,36] the prevalence of this feature in AIR is unknown. However, we observed hyperautofluorescent rings in all four cases that we examined and so we hypothesize that there is a high prevalence of this feature in AIR. The hyperautofluorescent rings in our series of patients are less intense than those observed in RP. This may be because of the short duration of disease in this rapidly progressing degeneration, and therefore, the ring may have not had time to develop further as it would in more long-standing conditions, such as RP. This study therefore suggests that hyperautofluorescent rings can be formed within a relatively short period of a few months.

Because there is no definitive way to make the diagnosis of AIR because of the lack of clinical standardization and autoantibody specificity, the presence of a hyperautofluorescent ring may contribute to the diagnosis of AIR in patients presenting with sudden or subacute loss of vision, ERG findings suggestive of AIR rather than RP, and associated anti-retinal antibody positivity. Our study is limited by the fact that it is a case series study with a small sample size. The frequency of the hyperautofluorescent ring in AIR patients will therefore be better determined by a larger study. Additionally, a study with more patient follow-up may provide data on the rate of ring constriction and IS–OS loss in these patients. However, long follow-up in cancer-associated retinopathy patients is difficult because they generally present with metastatic cancer and have a relatively short mean survival time.

The present study revealed the structure of a hyper-autofluorescent ring in four AIR patients using SD-OCT and demonstrated ring constriction in one of them. The use of FAF in conjunction with SD-OCT may help facilitate a timely and cost-efficient diagnosis of AIR through ERG and serology testing. Monitoring hyperautofluorescent ring constriction and IS–OS junction loss may help in tracking progression and response to treatment of these patients.

Acknowledgments

References

1. Solomon SD, Smith JH, O'Brien J. Ocular manifestations of systemic malignancies. Curr Opin Ophthalmol. 1999; 10:447–451. [PubMed: 10662250]

2. De Potter P. Ocular manifestations of cancer. Curr Opin Ophthalmol. 1998; 9:100–104. [PubMed: 10387328]

3. Adamus G, Ren G, Weleber RG. Autoantibodies against retinal proteins in paraneoplastic and autoimmune retinopathy. BMC Ophthalmol. 2004; 4:5. [PubMed: 15180904]

4. Hooks JJ, Tso MO, Detrick B. Retinopathies associated with antiretinal antibodies. Clin Diagn Lab Immunol. 2001; 8:853–858. [PubMed: 11527791]

5. Adamus G, Karren L. Autoimmunity against carbonic anhydrase II affects retinal cell functions in autoimmune retinopathy. J Autoimmun. 2009; 32:133–139. [PubMed: 19269136]

6. Heckenlively JR, Ferreyra HA. Autoimmune retinopathy: a review and summary. Semin Immunopathol. 2008; 30:127–134. [PubMed: 18408929]

7. Gass JD, Agarwal A, Scott IU. Acute zonal occult outer retinopathy: a long-term follow-up study. Am J Ophthalmol. 2002; 134:329–339. [PubMed: 12208243]

8. Jacobson SG, Morales DS, Sun XK, et al. Pattern of retinal dysfunction in acute zonal occult outer retinopathy. Ophthalmology. 1995; 102:1187–1198. [PubMed: 9097746]

9. Shimazaki K, Jirawuthiworavong GV, Heckenlively JR, et al. Frequency of anti-retinal antibodies in normal human serum. J Neuroophthalmol. 2008; 28:5–11. [PubMed: 18347451]

10. von Rückmann A, Fitzke FW, Bird AC. Distribution of fundus autofluorescence with a scanning laser ophthalmoscope. Br J Ophthalmol. 1995; 79:407–412. [PubMed: 7612549]

11. Heckenlively JR, Jordan BL, Aptsiauri N. Association of anti-retinal antibodies and cystoid macular edema in patients with retinitis pigmentosa. Am J Ophthalmol. 1999; 127:565–573. [PubMed: 10334350]

12. Tamm SA, Whitcup SM, Gery I, et al. Immune response to retinal antigens in patients with gyrate atrophy and other hereditary retinal dystrophies. Ocul Immunol Inflamm. 2001; 9:75–84. [PubMed: 11449323]

13. von Rückmann A, Fitzke FW, Bird AC. Distribution of pigment epithelium autofluorescence in retinal disease state recorded in vivo and its change over time. Graefes Arch Clin Exp Ophthalmol. 1999; 237:1–9. [PubMed: 9951634]

14. Delori FC, Staurenghi G, Arend O, et al. In vivo measurement of lipofuscin in Stargardt's disease —fundus flavimaculatus. Invest Ophthalmol Vis Sci. 1995; 36:2327–2331. [PubMed: 7558729]

15. Holz FG, Bellman C, Margaritidis M, et al. Patterns of increased fundus autofluorescence in the junctional zone of geographic atrophy of the retinal pigment epithelium associated with age related macular degeneration. Graefes Arch Clin Exp Ophthalmol. 1999; 237:145–152. [PubMed: 9987631]

16. Kurz-Levin MM, Halfyard AS, Bunce C, et al. Clinical variations in assessment of bull's-eye maculopathy. Arch Ophthalmol. 2002; 120:567–575. [PubMed: 12003605]

17. Eldred GE, Katz ML. Fluorophores of the human retinal pigment epithelium: separation and spectral characterization. Exp Eye Res. 1988; 47:71–86. [PubMed: 3409988]

18. Kennedy CJ, Rakoczy PE, Constable IJ. Lipofuscin of the retinal pigment epithelium: a review. Eye. 1995; 9:763–771. [PubMed: 8849547]

19. Robson AG, Saihan Z, Jenkins SA, et al. Functional characterization and serial imaging of abnormal fundus autofluorescence in patients with retinitis pigmentosa and normal visual acuity. Br J Ophthalmol. 2006; 90:472–479. [PubMed: 16547330]

20. Lima LH, Cella W, Greenstein VC, et al. Structural analysis of hyperautofluorescent ring in patients with retinitis pigmentosa. Retina. 2009; 29:1025–1031. [PubMed: 19584660]

21. Robson AG, Michaelides M, Luong VA, et al. Functional correlates of fundus autofluorescence abnormalities in patients with RPGR or RIMS1 mutations causing cone or cone-rod dystrophy. Br J Ophthalmol. 2008; 92:95–102. [PubMed: 17962389]

22. Tsang SH, Vaclavik V, Bird AC, et al. Novel phenotypic and genotypic findings in X-linked retinoschisis. Arch Ophthalmol. 2007; 125:259–267. [PubMed: 17296904]

23. Scholl HP, Chong NH, Robson AG, et al. Fundus autofluorescence in patients with leber congenital amaurosis. Invest Ophthalmol Vis Sci. 2004; 45:2747–2752. [PubMed: 15277500]

24. Marmor MF, Fulton AB, Holder GE, et al. ISCEV Standard for full-field clinical electroretinography (2008 update). Doc Ophthalmol. 2009; 118:69–77. [PubMed: 19030905]

25. Hartong DT, Berson EL, Dryja TP. Retinitis pigmentosa. Lancet. 2006; 368:1795–1809. [PubMed: 17113430]

26. Milam AH, Curcio CA, Cideciyan AV, et al. Dominant late-onset retinal degeneration with regional variation of sub-retinal pigment epithelium deposits, retinal function, and photoreceptor degeneration. Ophthalmology. 2000; 107:2256–2266. [PubMed: 11097607]

27. Weleber RG, Watzke RC, Shults WT, et al. Clinical and electrophysiologic characterization of paraneoplastic and autoimmune retinopathies associated with antienolase antibodies. Am J Ophthalmol. 2005; 139:780–794. [PubMed: 15860281]

28. Khan N, Huang JJ, Foster CS. Cancer associated retinopathy (CAR): an autoimmune-mediated paraneoplastic syndrome. Semin Ophthalmol. 2006; 21:135–141. [PubMed: 16912011]

29. Adamus G, Brown L, Weleber RG. Molecular biomarkers for autoimmune retinopathies: significance of anti-transducin-alpha autoantibodies. Exp Mol Pathol. 2009; 87:195–203. [PubMed: 19744478]

30. Murakami T, Akimoto M, Ooto S, et al. Association between abnormal autofluorescence and photoreceptor disorganization in retinitis pigmentosa. Am J Ophthalmol. 2008; 145:687–694. [PubMed: 18242574]

31. Ergun E, Hermann B, Wirtitsch M, et al. Assessment of central vision function in Stargardt's disease/fundus flavimaculatus with ultra-high resolution optical coherence tomography. Invest Ophthalmol Vis Sci. 2005; 46:310–316. [PubMed: 15623790]

32. Witkin AJ, Ko TH, Fujimoto JG, et al. Ultra-high resolution optical coherence tomography assessment of photoreceptors in retinitis pigmentosa and related diseases. Am J Ophthalmol. 2006; 142:945–952. [PubMed: 17157580]

33. Horio N, Kachie S, Hori K, et al. Progressive change of optical coherence tomography scans in retinal degeneration slow mice. Arch Ophthalmol. 2001; 119:1329–1332. [PubMed: 11545639]

34. Huang Y, Cideciyan AV, Papastergiou GI, et al. Relation of optical coherence tomography to microanatomy in normal and rd chickens. Invest Ophthalmol Vis Sci. 1998; 39:2405–2416. [PubMed: 9804149]

35. Ling CP, Pavesio C. Paraneoplastic syndromes associated with visual loss. Curr Opin Ophthalmol. 2003; 14:426–432. [PubMed: 14615650]

36. Wakabayashi T, Sawa M, Gomi F, et al. Correlation of fundus autofluorescence with photoreceptor morphology and functional changes in eyes with retinitis pigmentosa. Acta Ophthalmol. 2010; 88:177–183.
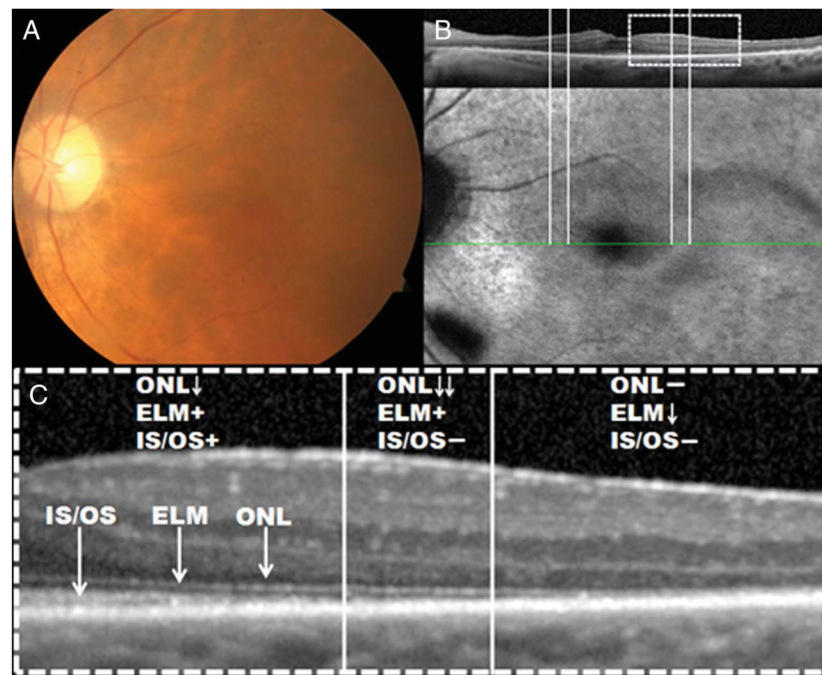
Fig. 1.
A. Color fundus photograph of the left eye of Patient 1, diagnosed with cancer-associated retinopathy, showed mild RPE atrophy and retinal artery narrowing but no pigment deposits. **B.** Fundus autofluorescence along with the corresponding SD-OCT revealed a parafoveal hyperautofluorescent ring. Fundus autofluorescence appears normal inside the ring of surviving retina and abnormal outside the ring. **C.** The magnified SD-OCT scan revealed that across the ring, there was loss of photoreceptor IS–OS junction and thinning of the ONL. Outside the hyperautofluorescent ring, there was loss of IS–OS junction, ELM, and ONL. Inside the ring, all retinal layers were observed, but there was thinning of the IS–OS junction, ONL, and photoreceptor outer segment layer as they approached the inner border of the ring.
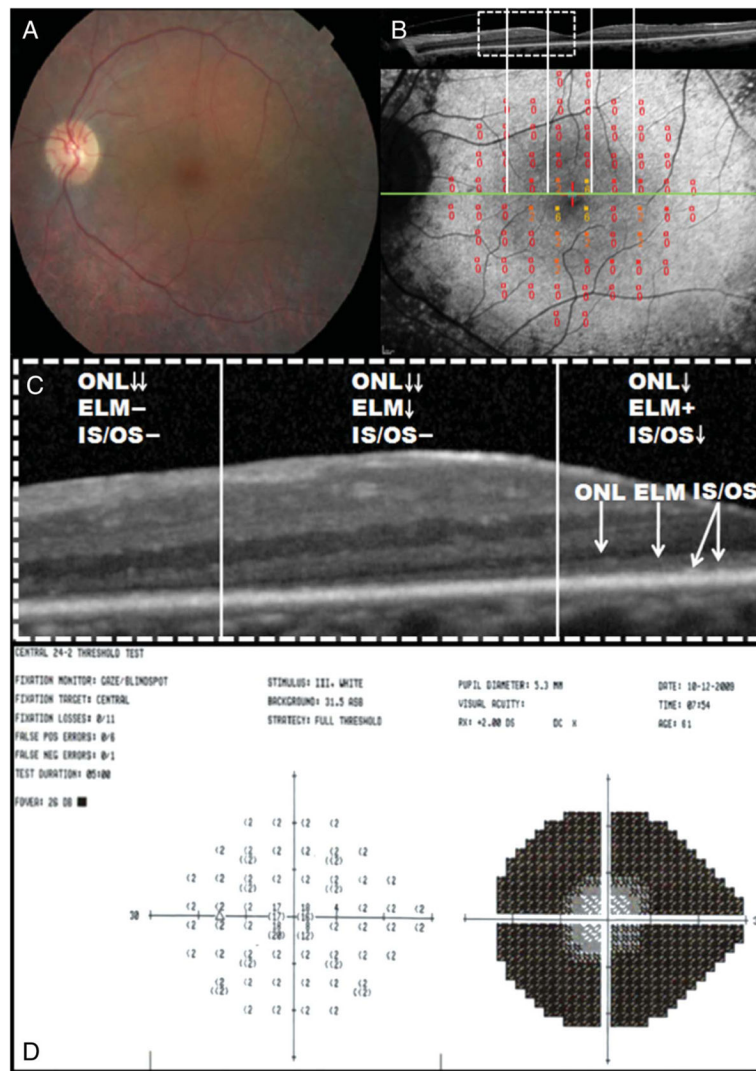
Fig. 2.
A. Color fundus photograph of the left eye of Patient 2, diagnosed with AIR, showed RPE mottling and optic disc pallor but no pigment deposits. **B.** Fundus autofluorescence along with the corresponding SD-OCT revealed a parafoveal hyperautofluorescent ring. Fundus autofluorescence appears normal inside the ring of surviving retina and abnormal outside the ring. The MP1 demonstrated a marked decrease in sensitivity at the inner border of the ring and sensitivity was non-recordable outside the ring. Inside the ring, the sensitivity was also decreased. **C.** The magnified SD-OCT scan revealed that across the ring, there was loss of IS–OS junction, ELM disorganization, and ONL thinning. Outside the hyperautofluorescent ring, there was loss of IS–OS junction and ELM and further thinning of ONL. Within the hyperautofluorescent ring, the retinal layers were generally intact, but there was discontinuity of IS–OS junction and thinning of the ONL and photoreceptor outer segment layer. **D.** The 24-2 HVF showed extensive ring scotoma with decreased sensitivity in the central area. Foveal sensitivity was also decreased (26 dB).
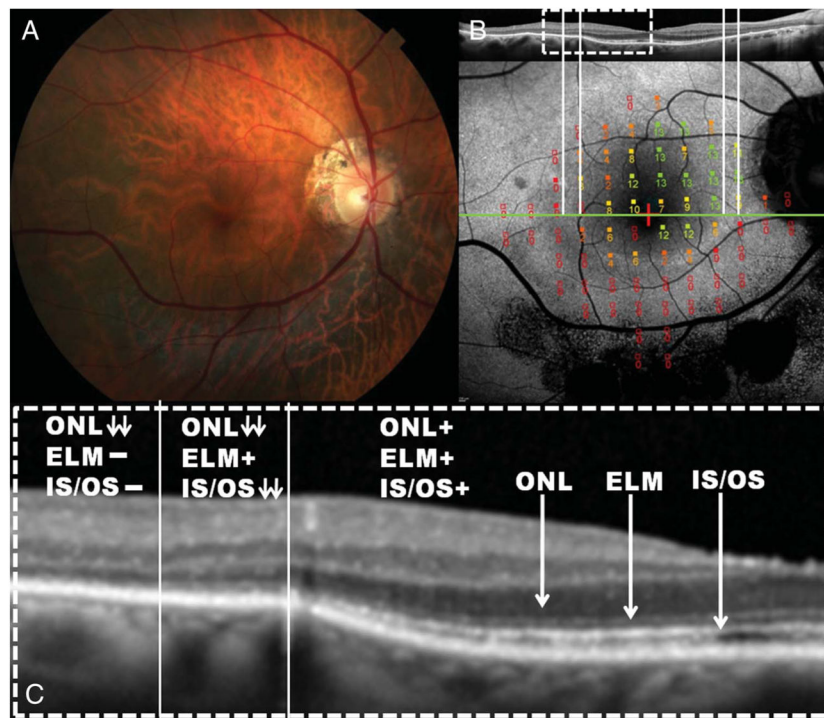
Fig. 3.
A. Color fundus photograph of the right eye of Patient 3, diagnosed with AIR, showed moderate RPE atrophy with retinal artery narrowing but no pigment deposits. **B.** Fundus autofluorescence along with the corresponding SD-OCT revealed a parafoveal hyperautofluorescent ring. Fundus autofluorescence appears normal inside the ring of surviving retina and abnormal outside the ring. The MP1 demonstrated a decreased sensitivity within the hyperautofluorescent ring, and there was an additional decrease starting at the inner border of the ring. Sensitivity was nonrecordable outside the ring. **C.** The magnified SD-OCT scan revealed that across the ring, there was IS–OS junction loss and ONL thinning. The retinal structure was generally intact within the hyperautofluorescent ring, but there was thinning of the ONL and photoreceptor outer segment layer and some disruption of the IS–OS junction toward the inner boundary of the ring. Outside the hyperautofluorescent ring, there was loss of IS–OS junction and ELM, as well as further thinning of ONL.
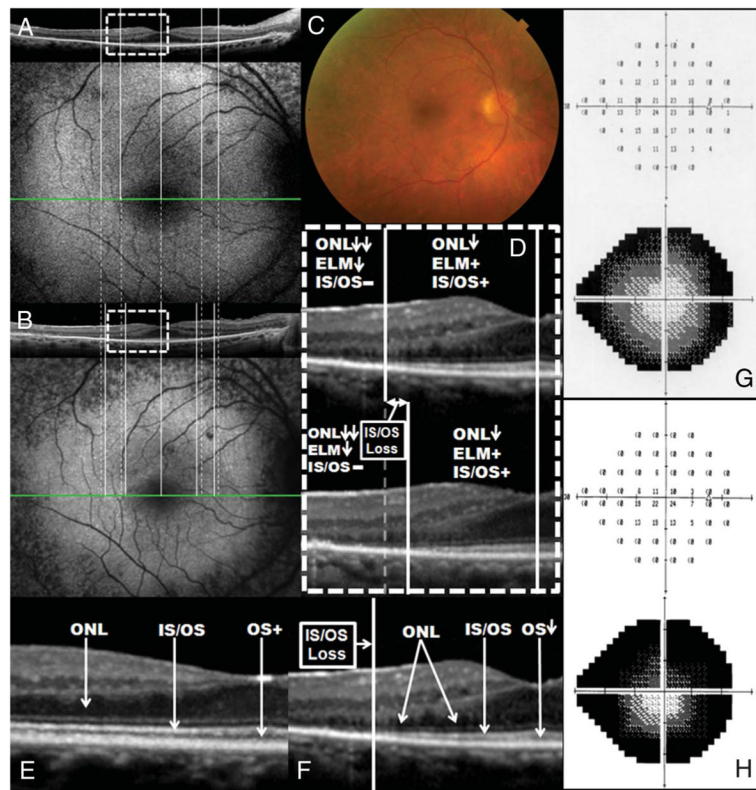
Fig. 4.
A. Baseline FAF along with the corresponding SD-OCT of the right eye of Patient 4 revealed a parafoveal hyperautofluorescent ring. **B.** Three years later, FAF along with the corresponding SD-OCT showed constriction of both the inner and the outer borders of the hyperautofluorescent ring. **C.** Color fundus photograph showed mild RPE mottling in the posterior pole and retinal periphery but no pigment deposits. **D.** The magnified SD-OCT scans revealed that across the ring, there was IS–OS junction and ELM loss and thinning of ONL. Inside the ring, all retinal layers were observed, but there was thinning of the IS–OS junction, ONL, and photoreceptor outer segment layer as they approached the inner border of the ring. Note the loss of IS–OS junction between the first visit (top) and the most recent visit (bottom). **E.** The magnified SD-OCT scan of a normal control eye with normal ONL, IS–OS junction, and photoreceptor outer segments. **F.** When compared with the control eye, the magnified SD-OCT scan of Patient 4 revealed thinning of the ONL and photoreceptor outer segment layer and disruption of the IS–OS junction toward the inner boundary of the ring. **G.** The baseline 24-2 HVF showed a dense ring scotoma that enlarged 3 years later (H).
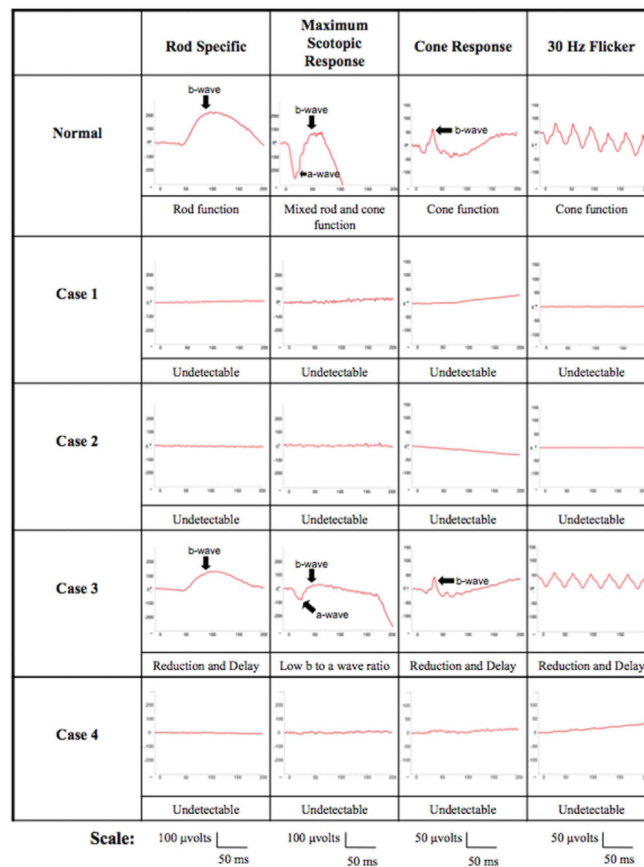
Fig. 5.

The top row shows an International Society for Clinical Electrophysiology of Vision standardized full-field ERG tracing for the rod-specific response, maximum scotopic response, cone response, and 30-Hz flicker of a normal subject. Patients 1, 2, and 4 had nondetectable scotopic and photopic full-field ERGs. Patient 3 had reduced and delayed scotopic and photopic responses: scotopic rod-specific ERG b-wave amplitudes were 141 μV in the right eye and 122 μV in the left eye. Maximal ERG a- and b-wave amplitudes were 147 μV and 195 μV in the right eye and 80 μV and 110 μV in the left eye. Transient photopic ERG had b-wave amplitudes and implicit times of 101 μV and 33 milliseconds in the right eye and 59 μV and 33 milliseconds in the left eye. Photopic 30-Hz flicker ERG had implicit times and amplitudes of 31 milliseconds and 63 μV in the right eye and 30 milliseconds and 60 μV in the left eye.
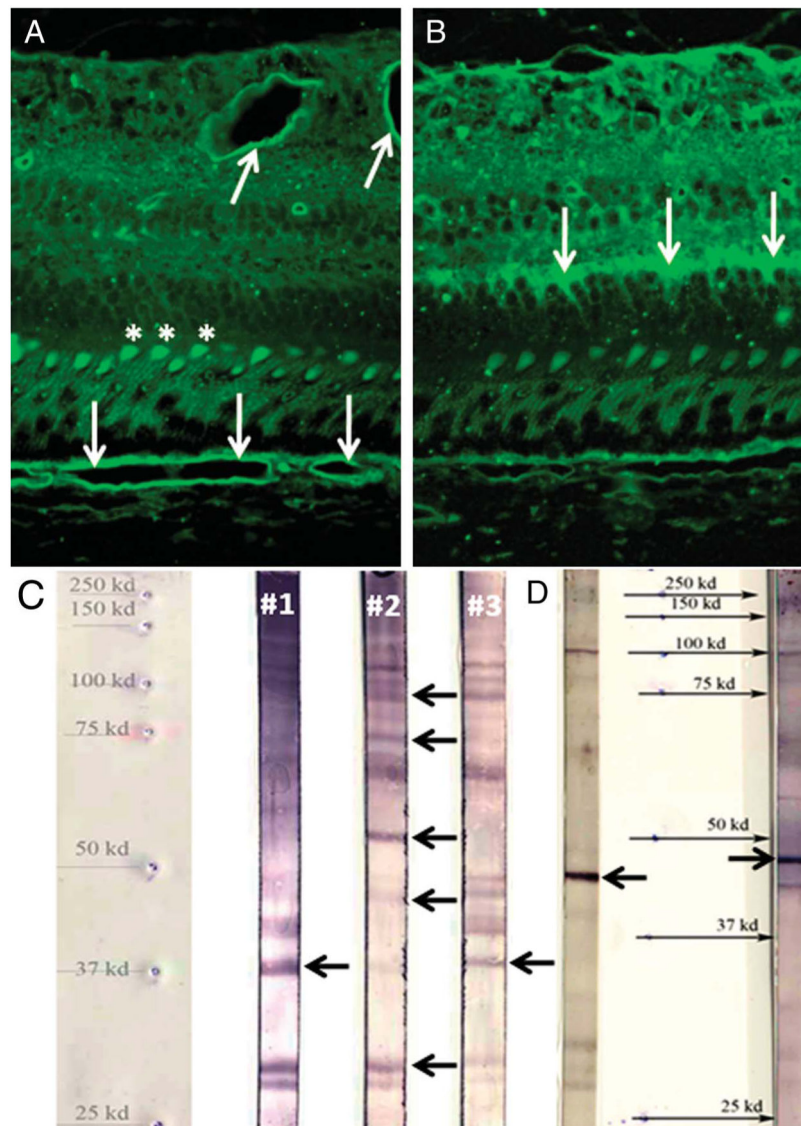
Fig. 6.
Immunohistochemistry and immunoblot analyses of the serum reactivity in study patients.
A. Immunohistochemistry of Patient 2 showed reactivity against the outer segments (asterisks) and the retinal and choroidal vascular beds (arrows) of a primate specimen. **B.** Immunohistochemistry of Patient 3 revealed reactivity against the outer plexiform layer (arrows) of a primate specimen. **C.** Immunoblot analysis of Patients 1 and 3 demonstrated reactivity against 40-kDa outer plexiform layer protein (arrows) and against 33-, 45- (outer segments), 55- (vascular bed), 64-, 72-, and 90-kDa proteins for Patient 2 (arrows). **D.** Immunoblot analysis of Patient 4 (left: retina reaction; right: RPE reaction) showed reactivity against 47-kDa protein (arrows).